Supplemental Materials

Molecular Biology of the Cell

Beaudet et al.

Figure S1. Related to Figure 1. Anillin has different cortical dynamics during early vs. late ingression. (A) Cartoon cells show how the stage of ingression was determined by the ratio of the length of the ingressed cortex 'B' over the width of the cell at the equator 'A'; where $R > 0.6$ was 'early' and $R < 0.6$ was 'late'. (B) Timelapse images show FRAP of HeLa cells expressing mCherry:Tubulin (magenta) and GFP:Anillin (full-length; green) during early or late ingression. The boxed insets show the ROI's that were photobleached in Fire LUTs. The scale bars are 10 μm or 2 μm for boxed insets. Indicated times are before (-) or after (+) photobleaching. (C) A graph shows the fraction of fluorescence recovery (Y-axis) over time (X-axis, seconds) for anillin during early (n=31) and late (n=15) ingression. Bars show standard deviation (SD). The table shows the maximum recovery (y_{max}), recovery time constant (τ) and half-life ($\tau_{1/2}$) of anillin during early and late ingression. Standard errors are shown in parentheses (SEM).

Figure S2. Related to Figure 2. The microtubule-binding region partially overlaps with the C-terminal NLS. (A) Immunoblots of the pulldown assays from Figure 2A showing GST-tagged importin-β (Imp-β) with MBP or MBP-tagged C2 domain (Ctl) vs. NLS mutant (NLS) are shown with corresponding Ponseau S-stained blots for total protein levels. (B) Coomassie-stained gels show co-sedimentation assays using 1.5 μM purified microtubules (MTs) with 1.5 μM MBP-tagged anillin C2 (top) or NLS mutant (bottom; S, supernatants; P, pellets). The table shows their mean binding capacity and dissociation coefficients (Kd), along with the SD. The graph shows bound anillin C2 (μM; Y-axis) plotted against free microtubules (μM; X-axis). Bars show SD (n=3 replicates). (C) A Coomassie-stained gel shows co-sedimentation assays using 1.5 μM purified MTs incubated with 1.5 μM MBP-tagged anillin C2 and 0-1.5 μM GST-tagged importin-β (S, supernatants; P, pellets). The bar graph shows the ratio of anillin (C2) in the supernatant (S) vs. bound (pellet; P) for the indicated concentrations (μM) of GST:Importin-β. Bars show SD (n=3 replicates). Data was analyzed and p values were determined by the unpaired Student's *t* test (n.s. not significant, *$p < 0.05$). (D) Immunoblots show PIP (phospholipid) strips incubated with purified GST, GST-tagged anillin (AHD) control, NLS mutant, or *strong* I/F mutant protein as indicated. The schematic shows the corresponding location for each type of lipid on the strips.

Figure S3. Related to Figure 3. Importin-binding is regulated by active RhoA. (A-E) Immunoblots of the pull-down assays from Figure 3A-D are shown with their corresponding Ponceau S-stained blots below for total protein levels. A) Immunoblots show *in vitro* binding of purified GST or GST-tagged importin-β (Imp-β) with MBP-tagged C-terminus of anillin (C-term; top) or the C2 domain (bottom). (B) An immunoblot shows a pull down of GFP-tagged C-terminus of anillin (C-term) from HeLa cell lysates with purified GST or GST-tagged importin-β. (C) An immunoblot as in (B), but where cell lysates were preloaded with 5 mM GDP or 5 mM GTP as indicated. (D) An immunoblot shows pull downs of GFP-tagged importin-β from lysates from cells overexpressing (O/E) Myc-tagged Ect2 C-terminus to generate active RhoA (left), or after Ect2 RNAi to reduce active RhoA (right), with purified MBP or MBP-tagged anillin (RBD + C2). (E) Immunoblots show pull downs of GFP-tagged importin-β from lysates as in (D) with MBP, MBP-tagged anillin (RBD + C2; Ctl) or with RBD mutations that disrupt RhoA-binding (A703E; E721A or A740E; E758A in the longer isoform; RBD), or mutations that strongly disrupt the RBD-C2 interface (735LL736 – DD or 772LL773 – DD in the longer isoform; strong I/F).

Figure S4. Related to Figures 5 and 6. The interface between the RBD and C2 domain is required to control cortical recruitment and cytokinesis. (A) A ribbon structure shows anillin RBD (magenta) + C2 domain (green) bound to RhoA-GTP (cyan). The boxed inset to the left shows a top down view of the RhoA-RBD (right) and RBD-C2 interfaces (left). Amino acids on the αB coil of the RBD form a hydrophobic interaction with amino acids within the disordered loop between the β2 and β3 strands in the C2 domain. The boxed inset (top right) shows amino acids within the αA and αB helices of the RBD that are predicted to be essential for RhoA-GTP-binding (Sun et al., 2015). The boxed inset below shows a zoomed in region of the interface between the RBD and C2 domain. Indicated are the positions of amino acids on the αB coil that form hydrophobic interactions with the disordered loop between the β2 and β3 strands in the C2 domain. (B) Images of fixed interphase HeLa cells immuno-stained for GFP show how anillin was determine to be nuclear vs. cytosolic. The average levels in the red square (nucleus) were calculated as a ratio R vs. the average levels in the yellow square (cytosol). If $R > 1.25$, anillin was determined to be nuclear, while $R < 1.25$ was cytosolic. (C) Immunoblots show pull downs of GFP-tagged RhoA from lysates with MBP or MBP-tagged anillin (RBD + C2), either control (Ctl), I/F + NLS mutant, or *strong* I/F mutant. The corresponding Ponceau-S stained blot is below to show the total protein.

A

B

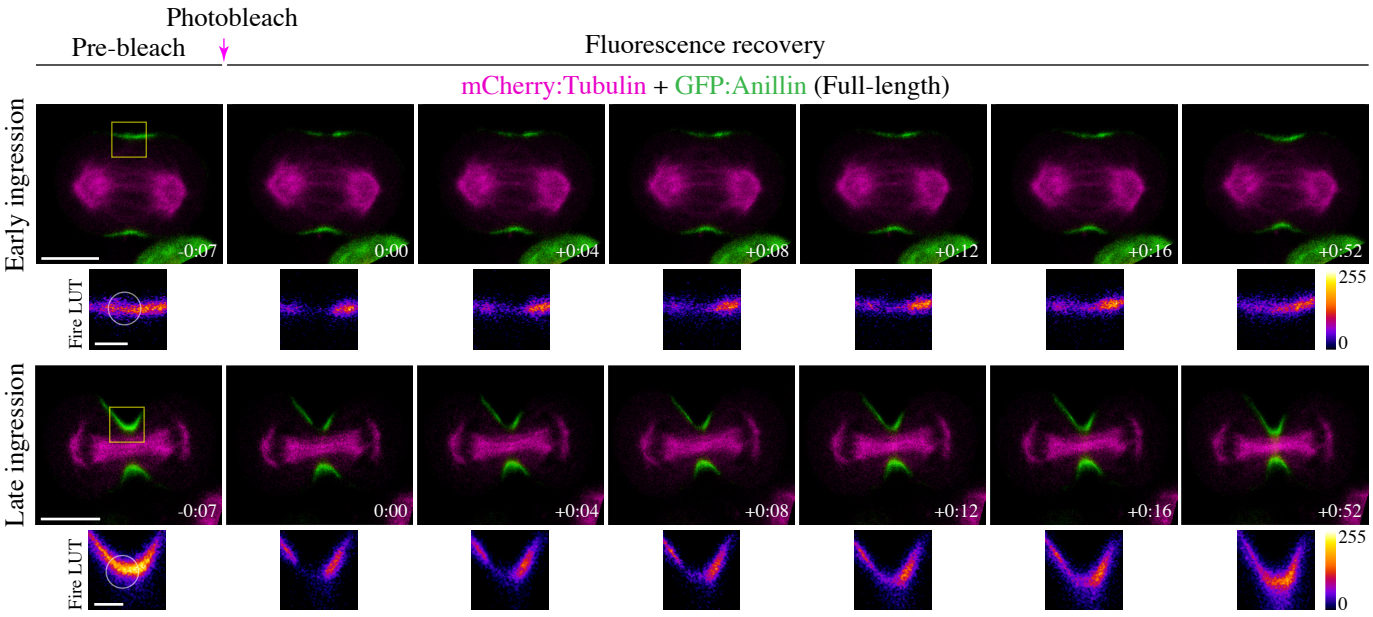

C

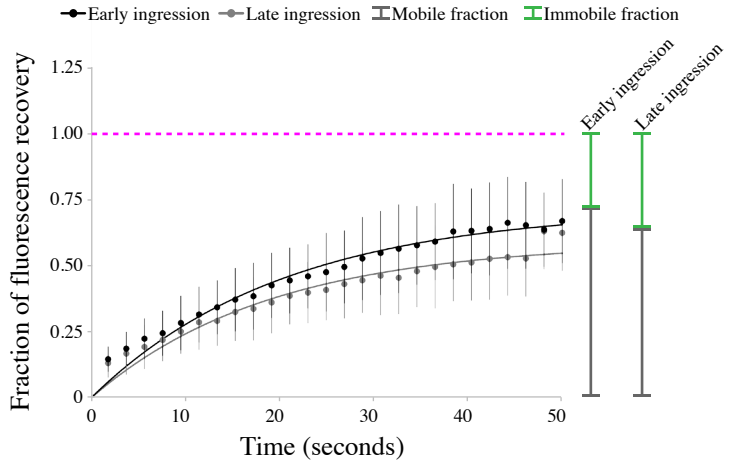

	Early ingression	Late ingression
y_{max}	0.723 (0.021)	0.595 (0.024)
τ (s^{-1})	0.047 (0.003)	0.051 (0.005)
$\tau_{1/2}$ (s)	14.70	13.61

Figure S1

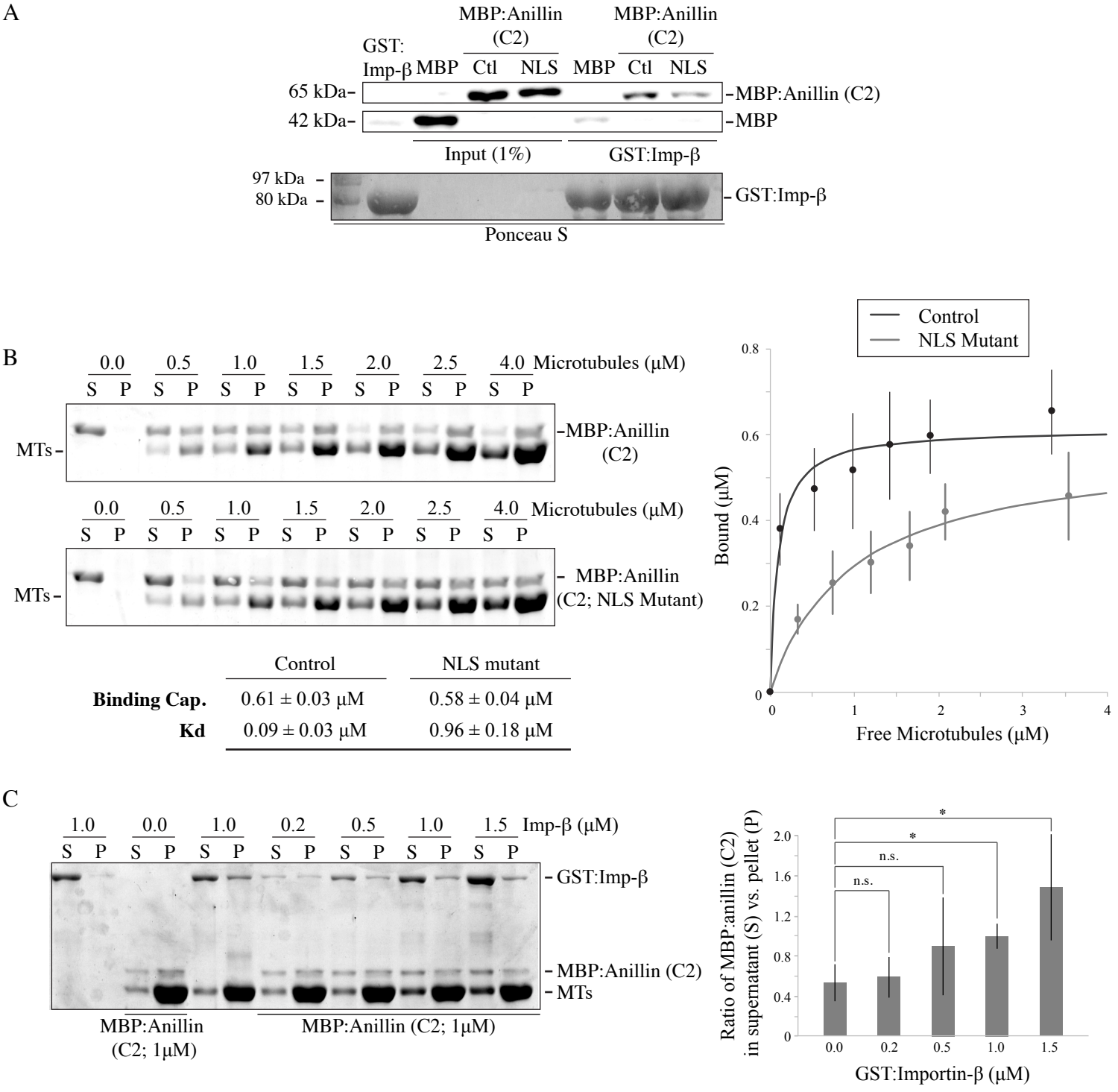
A
MBP:Anillin (C2)
MBP:Anillin (C2)
GST: Imp-β
MBP
Ctl
NLS
MBP
Ctl
NLS
65 kDa
MBP:Anillin (C2)
42 kDa
MBP
Input (1%)
GST:Imp-β
97 kDa
80 kDa
GST:Imp-β
Ponceau S
B
0.0 0.5 1.0 1.5 2.0 2.5 4.0 Microtubules (μM)
S P S P S P S P S P S P S P
MTs
MBP:Anillin (C2)
MBP:Anillin (C2; NLS Mutant)
Control
NLS Mutant
Bound (μM)
Free Microtubules (μM)
Control
NLS mutant
Binding Cap.
0.61 ± 0.03 μM
0.58 ± 0.04 μM
Kd
0.09 ± 0.03 μM
0.96 ± 0.18 μM
C
1.0 0.0 1.0 0.2 0.5 1.0 1.5 Imp-β (μM)
S P S P S P S P S P S P S P
GST:Imp-β
MBP:Anillin (C2)
MTs
MBP:Anillin (C2; 1μM)
MBP:Anillin (C2; 1μM)
Ratio of MBP:anillin (C2) in supernatant (S) vs. pellet (P)
n.s.
n.s.
*
*
GST:Importin-β (μM)
D
GST:Anillin (AHD)
GST
Control
NLS Mutant
strong I/F Mutant
Lysophosphatidic Acid (LPA)
Lysophosphocholine (LPC)
PtdIns (PI)
PtdIns(3)P
PtdIns(4)P
PtdIns(5)P
Phosphatidylethanolamine (PE)
Phosphatidylcholine (PC)
Sphingosine-1-phosphate (S1P)
PtdIns(3,4)P2
PtdIns(3,5)P2
PtdIns(4,5)P2
PtdIns(3,4,5)P3
Phosphatidic Acid (PA)
Phosphatidylserine (PS)
Blue Blank

Figure S2

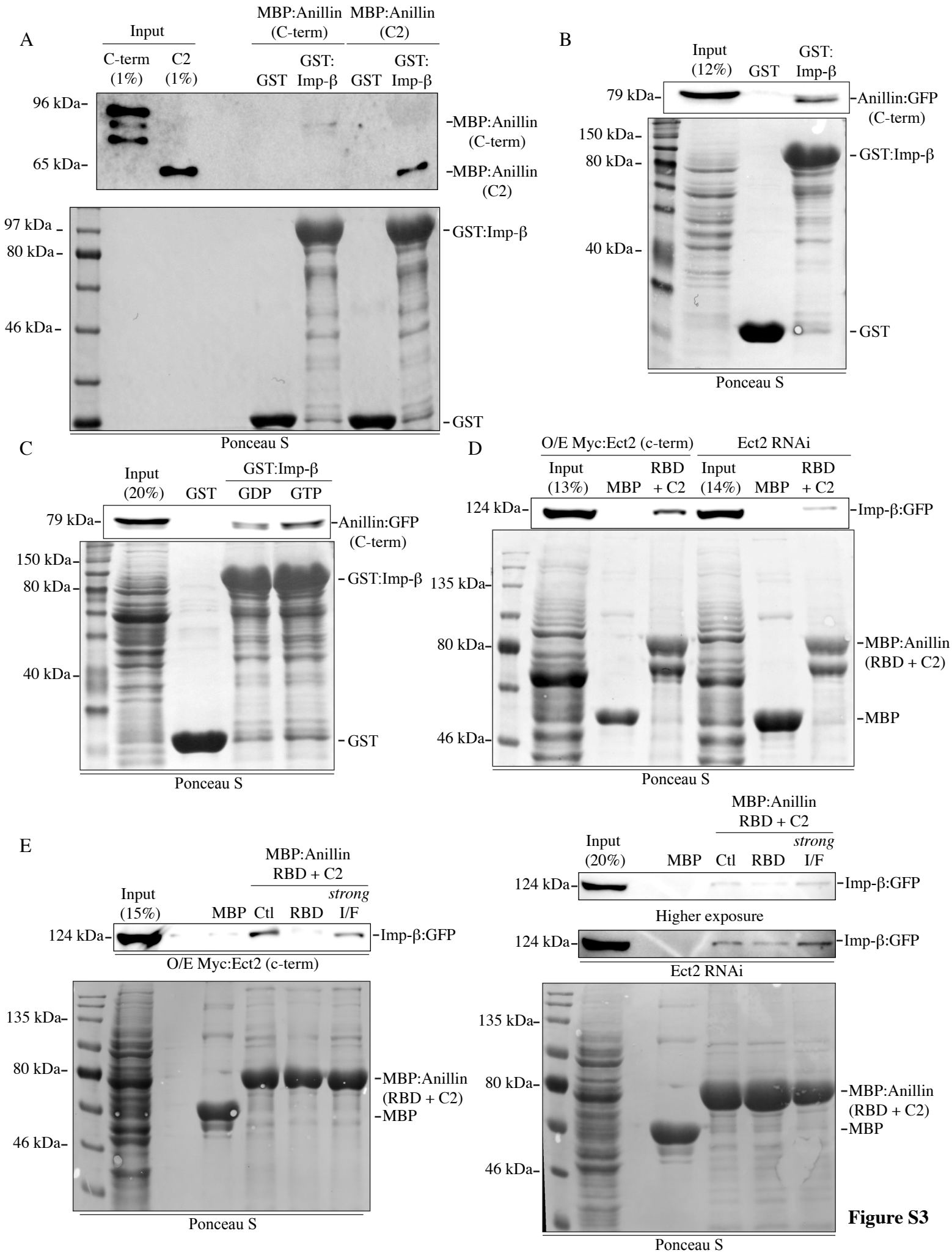
A
Input
C-term (1%)
C2 (1%)
MBP:Anillin (C-term)
MBP:Anillin (C2)
GST
GST: Imp-β
96 kDa
65 kDa
MBP:Anillin (C-term)
MBP:Anillin (C2)
97 kDa
80 kDa
46 kDa
GST:Imp-β
GST
Ponceau S
B
Input (12%)
GST
GST: Imp-β
79 kDa
Anillin:GFP (C-term)
150 kDa
80 kDa
40 kDa
GST:Imp-β
GST
Ponceau S
C
Input (20%)
GST
GST:Imp-β
GDP
GTP
79 kDa
Anillin:GFP (C-term)
150 kDa
80 kDa
40 kDa
GST:Imp-β
GST
Ponceau S
D
O/E Myc:Ect2 (c-term)
Ect2 RNAi
Input (13%)
MBP
RBD + C2
Input (14%)
MBP
RBD + C2
124 kDa
Imp-β:GFP
135 kDa
80 kDa
46 kDa
MBP:Anillin (RBD + C2)
MBP
Ponceau S
E
MBP:Anillin RBD + C2
strong
Input (15%)
MBP
Ctl
RBD
I/F
124 kDa
Imp-β:GFP
O/E Myc:Ect2 (c-term)
135 kDa
80 kDa
46 kDa
MBP:Anillin (RBD + C2)
MBP
Ponceau S
MBP:Anillin RBD + C2
strong
Input (20%)
MBP
Ctl
RBD
I/F
124 kDa
Imp-β:GFP
Higher exposure
124 kDa
Imp-β:GFP
Ect2 RNAi
135 kDa
80 kDa
46 kDa
MBP:Anillin (RBD + C2)
MBP
Ponceau S

Figure S3

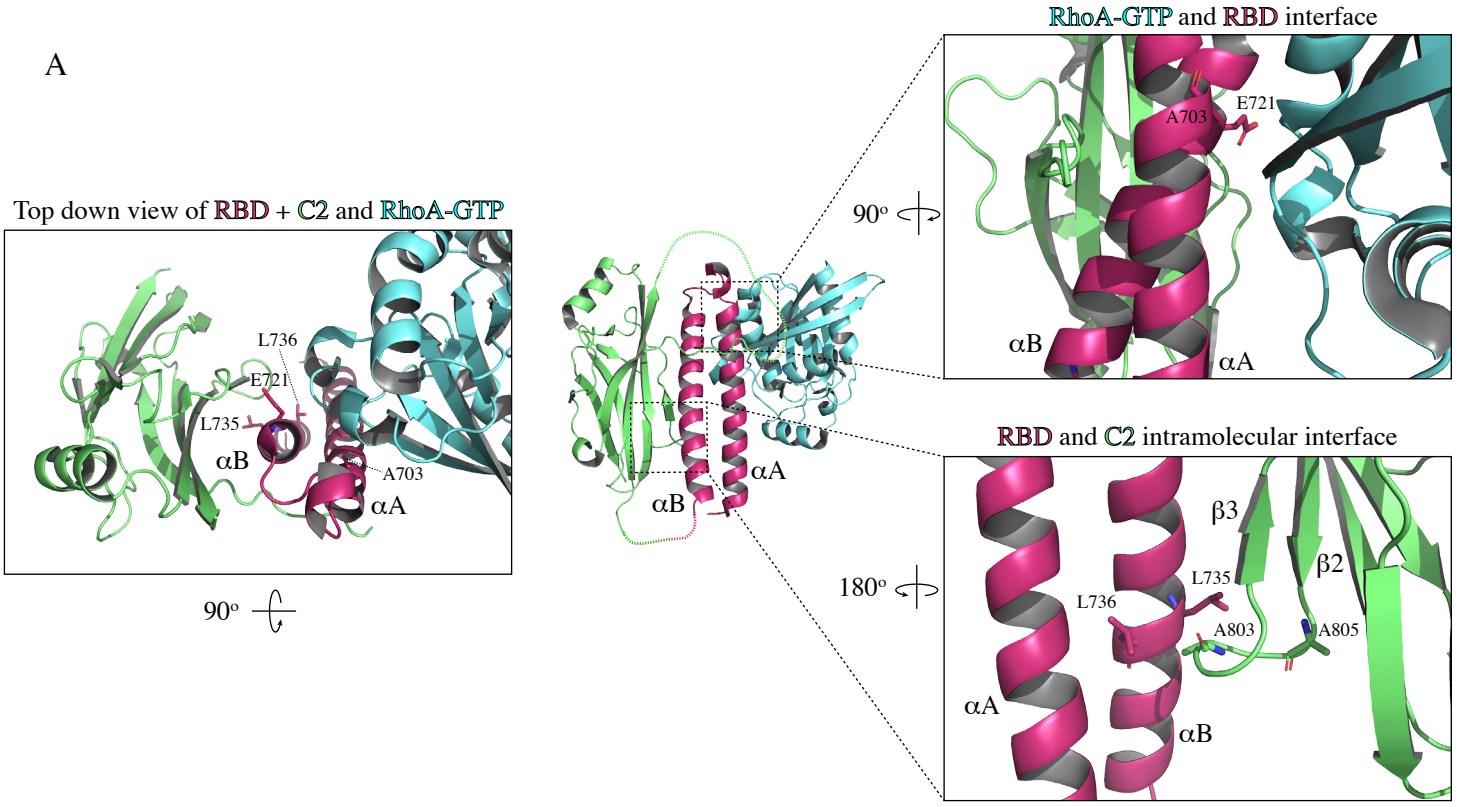
A
Top down view of RBD + C2 and RhoA-GTP
L736
E721
L735
αB
A703
αA
90°
RhoA-GTP and RBD interface
90°
A703
E721
αB
αA
RBD and C2 intramolecular interface
180°
β3
β2
L735
L736
A803
A805
αA
αB

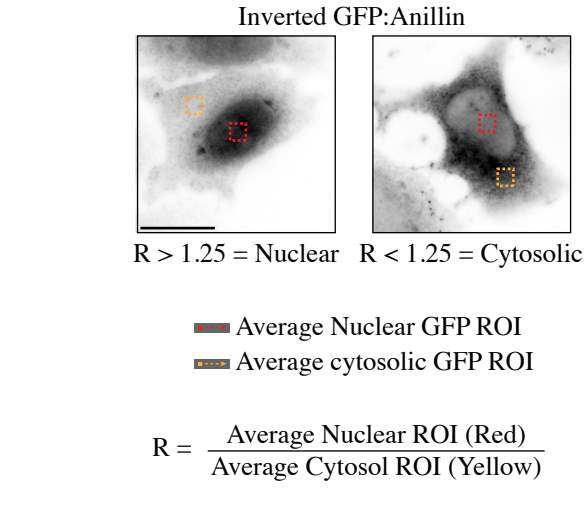
B
Inverted GFP:Anillin
R > 1.25 = Nuclear
R < 1.25 = Cytosolic
Average Nuclear GFP ROI
Average cytosolic GFP ROI
R = Average Nuclear ROI (Red) / Average Cytosol ROI (Yellow)

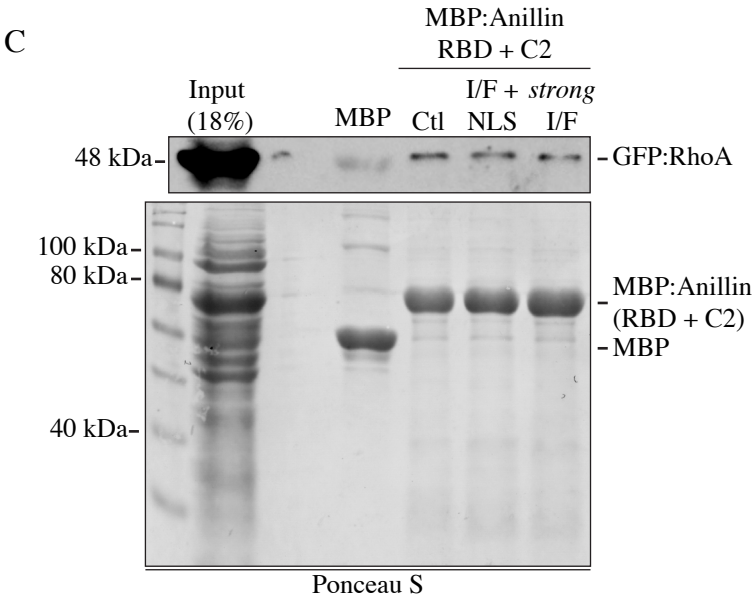
C
MBP:Anillin
RBD + C2
Input
(18%)
MBP
Ctl
I/F + strong
NLS
I/F
48 kDa
GFP:RhoA
100 kDa
80 kDa
40 kDa
MBP:Anillin
(RBD + C2)
MBP
Ponceau S

Figure S4